

Extraction of Maize Leaf Base and Inclination Angles Using Terrestrial Laser Scanning (TLS) Data

Lei Lei[✉], Zhenhong Li, Senior Member, IEEE, Jintao Wu[✉], Chengjian Zhang, Yaohui Zhu, Riqiang Chen, Zhen Dong, Hao Yang, and Guijun Yang

Abstract—Leaf base and inclination angles are two critical 3-D structural parameters in agronomy and remote sensing for breeding and modeling. Terrestrial laser scanning (TLS) has been proven to be a promising tool to quantify leaf base and inclination angles. However, previous TLS studies often focused on leaf base and inclination angles of certain trees or plants with flat leaves, such as European beech. Few studies have worked on leaf base and inclination angles of maize plants due to their curved and elongated characteristics. In this study, a machine learning-based [support vector machine (SVM)] method and a structure-based [skeleton extraction (SE)] method were presented to extract the leaf base and inclination angles of maize plants. After separating individual leaf points from the complete point cloud and skeleton points of maize plants and then extracting geometric features, the machine learning- and structure-based methods were used to calculate leaf base and inclination angles. Our results show that the leaf base and inclination angles extracted using these two methods agreed well with ground truth, and the estimation accuracy of the

machine learning-based method was obviously higher than that of the structure-based method. The mean absolute error (MAE), root-mean-squared error (RMSE), and relative RMSE (rRMSE) of the leaf base and inclination angles using the machine learning-based method were 4.56°, 6.17°, and 19.04% and 7.95°, 10.00°, and 20.24%, respectively; and those from the structure-based method were 6.22°, 7.47°, and 23.30% and 8.99°, 12.57°, and 25.85%, respectively. The machine learning-based method was also applied to a field with dense mature maize, and their MAE, RMSE, and rRMSE were 6.04°, 8.12°, and 25.90% and 11.30°, 13.52°, and 26.5%, respectively. It is demonstrated that both the machine learning- and structure-based methods are effective to estimate the leaf base and inclination angles of maize plants, although the machine learning-based method appears to outperform the structure-based method.

Index Terms—Leaf base angle, leaf inclination angle, machine learning-based method, structure-based method, terrestrial laser scanning (TLS).

I. INTRODUCTION

PLANT architecture can be defined as the shape, size, angle, and positional distributions of all the leaf elements [1]. It directly influences the biological and physical processes of a plant, such as photosynthesis and evapotranspiration [2]–[5].

The leaf angle of a plant contains two components: leaf base angle (stem–leaf angle) and leaf inclination angle. The leaf base angle is defined as the inclination between the midrib of the leaf blade and the vertical stem of a plant [6], [7]. The leaf base angle is the main trait that determines the compactness of a plant [8]. A smaller leaf base angle in maize decreases mutual shading and sustains light capture for photosynthesis even when there is increased plant density, thus improving the accumulation of leaf nitrogen for maize filling and increasing maize yield [8]–[11]. The leaf inclination angle is defined as the intersection angle between the normal vector of the center point of the leaf surface and the zenith direction [12]. Leaf inclination angle is an important plant structural trait, which influences the spectral reflectance and radiation transmission in plant canopy and, hence, interception, absorption, and photosynthesis. In addition, it is a fundamental parameter of radiative transfer models of plants at all scales [12], [13].

Various methods and instruments have been proposed over the years for measuring leaf angle [1], [5], [6], [14], [15].

Manuscript received April 22, 2021; revised October 12, 2021 and November 16, 2021; accepted January 8, 2022. Date of publication January 11, 2022; date of current version March 11, 2022. This work was supported in part by the National Key Research and Development Program of China under Grant 2021YFD2000102 and Grant 2017YFE0122500, in part by the Fundamental Research Funds for the Central Universities, Chang'an University, under Grant 300102260301 and Grant 300102261108, in part by the Shaanxi Province Science and Technology Innovation Team under Grant 2021TD-51, and in part by the European Space Agency through the ESA-MOST DRAGON-5 Project under Grant 59339. (Corresponding authors: Hao Yang; Guijun Yang.)

Lei Lei is with the College of Geological Engineering and Geomatics, Chang'an University, Xi'an 710054, China; also with the Big Data Center for Geosciences and Satellites (BDCGS), Xi'an 710054, China; and also with the Information Technology Research Center, Beijing Academy of Agriculture and Forestry Sciences, Beijing 100097, China (e-mail: leilei_ll@outlook.com).

Zhenhong Li is with the College of Geological Engineering and Geomatics, Chang'an University, Xi'an 710054, China; also with the Big Data Center for Geosciences and Satellites (BDCGS), Xi'an 710054, China; and also with the Key Laboratory of Western China's Mineral Resource and Geological Engineering, Ministry of Education, Xi'an 710054, China (e-mail: zhenhong.li@chd.edu.cn).

Jintao Wu is with the School of Computer and Software, Nanjing University of Information Science and Technology, Nanjing 210044, China (e-mail: ah_wjt@foxmail.com).

Chengjian Zhang, Yaohui Zhu, Riqiang Chen, Zhen Dong, and Hao Yang are with the Information Technology Research Center, Beijing Academy of Agriculture and Forestry Sciences, Beijing 100097, China (e-mail: 18210210075@stu.xust.edu.cn; yaohui_zhu@bjfu.edu.cn; chenriqiang1995@163.com; jmhsdz@163.com; yangh@nercita.org.cn).

Guojun Yang is with the Key Laboratory of Quantitative Remote Sensing in Agriculture of Ministry of Agriculture and Rural Affairs, Information Technology Research Center, Beijing Academy of Agriculture and Forestry Sciences, Beijing 100097, China (e-mail: yanggj@nercita.org.cn).

Digital Object Identifier 10.1109/TGRS.2022.3142205

Traditional measurements of leaf angle use tools, such as an inclinometer, compass, and protractor, which have the advantage of high precision, but are time-consuming, labor-intensive, and do not allow to achieve the high-throughput measurements required for phenotyping.

Some noncontact indirect and nondestructive methods of estimating the leaf angle have been investigated. Remote sensing is the most promising way to collect high-throughput measurements of leaf angle and the leaf angle was obtained mainly based on 2-D digital camera images. For example, Pisek *et al.* [16] and Ryu *et al.* [17] obtained the leaf inclination angle of leaves through the image analysis. Zhang *et al.* [18] extracted the leaf base angle traits of a single maize plant indoors using side- and top-view images. However, there are often strict requirements for the acquisition angle of the 2-D image, which limits its applicability. In the field of computer vision, the structure from motion (SFM) method makes it feasible to extract the leaf angle based on multiview imaging and 3-D reconstruction technology [19]. For example, after obtaining the 3-D point cloud of young wheat plants with the SFM method, Duan *et al.* [20] used a local polynomial regression fitting algorithm to fit the midrib of leaves and then extracted the leaf inclination angle. Dandrifosse *et al.* [21] used a binocular vision camera placed above the wheat canopy in the field to extract the leaf inclination angle distribution of the top leaves after fitting the plane through the Delaunay triangulation. Zermas *et al.* [22] reconstructed the 3-D canopies of corn plants using high-resolution RGB imagery with the SFM method and then obtained the leaf base angle of individual plants based on these 3-D reconstructed canopies.

In recent years, with the increased affordability and accuracy of light detection and ranging (LiDAR) measurements, the extraction of leaf angle based on terrestrial laser scanning (TLS) is becoming common [22]. Similar to the 3-D point cloud data obtained by the SFM method, there are two main methods for extracting the leaf angle based on TLS data: 1) skeleton extraction [18], [23]–[29] and 2) normal vector-based method [1], [12], [13], [30]–[33]. Wu *et al.* [25] used the Laplacian algorithm for skeleton extraction, which improved the accuracy of maize leaf base angle. Based on the Kinect point cloud, Xiang *et al.* [24] used the skeleton extraction-based method to separate stems from leaves and obtained the leaf base angle of indoor potted maize plants. The normal vector-based method assumes that the leaves are flat and that points cluster around a leaf using a nearest neighbors search around each point in the leaf cloud, e.g., using a fixed number of neighbors (kNN) for each point neighborhood [12], clustering is constrained by the leaf size [32], plane fitting based on the voxel method [30], plane clustering based on the *k*-means algorithm [34], [35], and plane fitting based on the convex hull algorithm [31]. The leaf inclination angle is then calculated using singular value decomposition or the principal component analysis method.

It should be noted that the normal vector-based method mainly targets flat and wide leaves, and therefore, it might not be optimal for elongated and curved leaves, such as those of maize. In addition, the “skeleton extraction” method focused

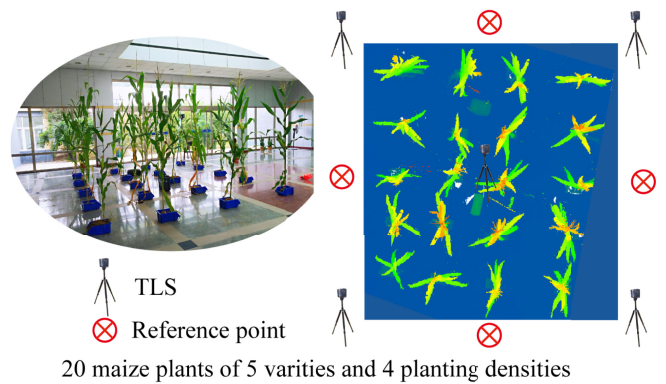


Fig. 1. (Left) Study area and scanning stations and (Right) reference points distribution.

on the leaf base angle, and few studies discussed the leaf inclination angle.

In the study, to overcome the limitations, we present two methods (i.e., a machine learning-based method and a structure-based method) to estimate the maize leaf base and inclination angles and then evaluate their performance with ground truth.

II. MATERIALS

A. Study Area

The study area is the National Experimental Station for Precision Agriculture in the Changping District of Beijing (40.18°N, 116.44°E). As shown in Fig. 1, a total of 20 maize plants of five varieties (A1-Zhengdan 958, A2-Xianyu 335, A3-Jing Nongke 728, A4-Chengdan 30, and A5-Jingpin 6) and four plant densities (45 000 plants/ha, 67 500 plants/ha, 90 000 plants/ha, and 105 000 plants/ha, with maize intervals of 15.6, 17.85, 22.73, and 35.71 cm, respectively) were selected from the field and were dug up, put into flowerpots and scanned indoors.

B. Data Collection

The study was conducted in the hall of the National Experimental Station for Precision Agriculture. The maize plants were in the spinning growth period (R1). A FARO Focus^s 350 (FARO Scanner Production GmbH Co.) was used to scan the 20 maize plants. The FARO Focus^s 350 laser scanner has a vertical field of view of -60° to 90° and a horizontal field of view of 0° – 360° . The scan distance is 20 m and the scanning accuracy is ± 1 mm, with a measurement rate of up to 976 000 points/s. Multistation scanning was used to obtain higher precision and higher density maize point clouds. The scan time per station was less than 2 min and 54 s. The five stations were located around and in the middle of the 20 maize plants. In order to achieve more accurate stitching of the five stations, a total of four reference points was arranged using chairs and instrument boxes. The stations and reference points were arranged, as shown in Fig. 1.

The data acquired in this experiment were used to quantitatively extract the leaf base and inclination angles of the

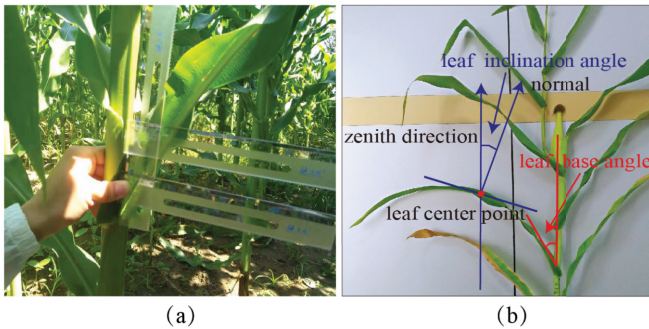


Fig. 2. Measurement of the real leaf base and inclination angles. (a) “F” ruler was used to measure the leaf base angle. (b) Measurement positions of the leaf base and inclination angles.

maize plants. Manual measurements (referred to as “ground truth”) with an “F” ruler were also taken to evaluate the accuracy of the extracted leaf base and inclination angles. As shown in Fig. 2(a), in order to obtain the ground truth with higher accuracy, two rulers were placed perpendicularly to each other, one at 5 cm and the other at 10 cm. The vertical ruler was based on the attachment of the leaf to the stem. The length of the leaf midrib was measured at 5 and 10 cm from the attachment on the stem, and the average leaf base angle was then calculated and considered as the ground truth. Because it is difficult to directly measure the leaf inclination angle from a maize plant, this parameter was measured from the point cloud data. The leaf center point was extracted from the leaf points, and the leaf inclination angle was measured from the leaf center point using the ImageJ software (<https://imagej.nih.gov/ij/>). A series of measurements were collected until three stable values were consecutively obtained, which should be close to each other, and then, the three values were averaged to estimate the leaf inclination angle. The measurement positions of the leaf base and inclination angles are shown in Fig. 2(b).

III. METHOD

A. Data Processing

1) *Data Preprocessing*: The FARO SCENE (V2019.0.0.1457, ITRILRI Company, Shandong, China) software was used to register and stitch together all the individual station data, with a stitching accuracy of 2–3 mm. FARO SCENE is a comprehensive 3-D point cloud processing and management tool for professional users, which can be used to view, manage, and analyze various 3-D scan data obtained from high-resolution 3-D laser scanners (such as FARO Focus^s 350 laser scanner). The SCENE software provides functions, such as automatic object recognition, scan data stitching, and positioning.

The scanning distance of the TLS was set to 20 m and this led to the fact that parts of the building were included in the scans. The stitched data were cropped with the LiDAR 360 (V4.0, GreenValley Company, Shanghai, China) software to remove the indoor buildings and other objects, as shown in Fig. 3(a).

Because the floor was flat and the flowerpots were all identical, the ground and flowerpot points were removed

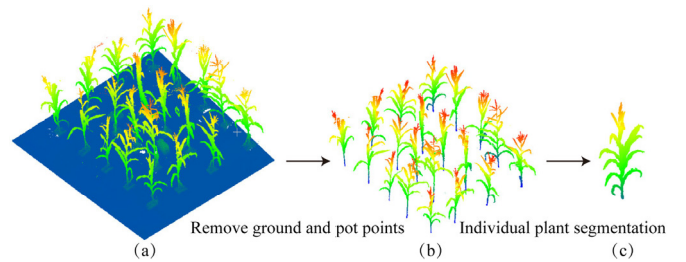


Fig. 3. Multistation scanning data stitching and data preprocessing. (a) Removing indoor buildings and other objects. (b) Removing ground and pot points. (c) Segmentation of the individual maize plant.

[Fig. 3(b)] using the height of the flowerpot. After the ground and flowerpot points were removed, the cropping tool in the LiDAR 360 software was used to segment the individual maize plants [Fig. 3(c)].

2) *Point Cloud Thinning*: Multistation scanning can yield high-precision point cloud data; however, it also increases the density of the measurements. The number of individual maize plant points reached about 400 000 on average. Although this allows to explore the detailed characteristics of maize plants, the processing efficiency is greatly reduced due to the excessive amount of point cloud data. In this study, a voxel-based thinning method was developed to thin high-density point cloud data, which not only reduces the point cloud density but can also be used to denoise without losing detailed characteristics of the maize plants. The main steps of the voxel-based method are given as follows.

The voxel-based method used for thinning high-density point cloud data includes the following main parts.

- 1) Voxelization of the point cloud data and calculation of the coordinates of the center point (x_i, y_j, z_k) of each voxel according to (1) and (2).
- 2) Calculation of the distance (d) between each point (x, y, z) and the center of each voxel (x_i, y_j, z_k) and determination of which voxel the point belongs to, as shown in (3).
- 3) Count of the number of points in each voxel, according to the analysis of point cloud distribution; if the number of points in a voxel is smaller than a threshold, the points in the voxel are considered to be noise points and will be deleted.
- 4) Adoption of the method of random selection, retaining part of the number of points in the remaining voxels, and completion of the point cloud thinning

$$\begin{cases} \text{rows} = (x_{\max} - x_{\min})/\text{voxelstep} \\ \text{cols} = (y_{\max} - y_{\min})/\text{voxelstep} \\ \text{heis} = (z_{\max} - z_{\min})/\text{voxelstep} \end{cases} \quad (1)$$

$$\begin{cases} x = x_{\min} + (i - 0.5) * \text{voxelstep} & \text{rows} \geq i \geq 1 \\ y = y_{\min} + (j - 0.5) * \text{voxelstep} & \text{cols} \geq j \geq 1 \\ z = z_{\min} + (k - 0.5) * \text{voxelstep} & \text{heis} \geq k \geq 1 \end{cases} \quad (2)$$

$$d = \sqrt{(x - x_i)^2 + (y - y_j)^2 + (z - z_k)^2} \quad (3)$$

where voxelstep is the voxel size, and the point cloud is grouped into rows \times cols \times heis voxels. x_{\max} , x_{\min} , y_{\max} , y_{\min} ,

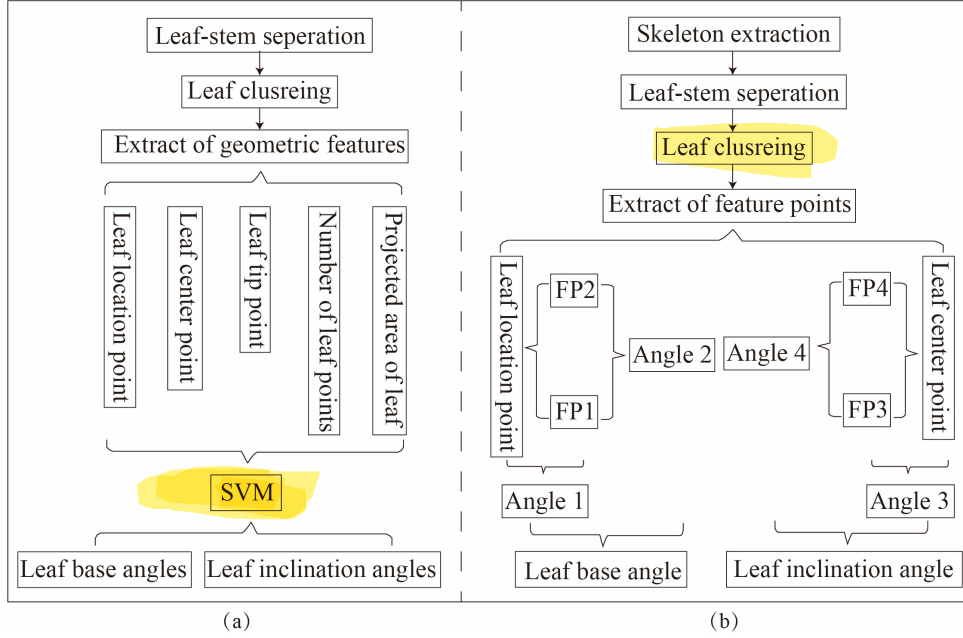


Fig. 4. Estimation of leaf base and inclination angles. (a) Machine learning-based method. (b) Structure-based method.

z_{\max} , and z_{\min} are the maximum and minimum coordinates of each point.

B. Extraction of Leaf Base and Inclination Angles

A machine learning-based [support vector machine (SVM)] method and a structure-based [skeleton extraction (SE)] method were employed to extract leaf base and inclination angles in this study.

SVM is a supervised nonparametric statistical learning technique [32], which can achieve good results even with small training datasets and a high-dimensional feature space [36]. The SVM.SVR in the sklearn library is used in the study for regression and prediction with a linear function being the kernel function. To obtain the best performance, the penalty parameter is set to 1.0 and the ϵ -insensitive loss function is set to “epsilon_insensitive”. In the machine learning-based method [Fig. 4(a)], after leaf-stem separation and leaf clustering, we extracted five geometric features (i.e., leaf location point, leaf center point, leaf tip point, number of leaf points, and projected area of the leaf) to predict leaf base and inclination angles. In this study, 20 maize plants were selected, yellow and dry leaves of the lowest layers and leaves that broke in the process of moving the plants were removed, and the total number of leaves was 179. We randomly selected 70% of all the samples as the training set and the remaining 30% as the predicted set and compare the predicted result with the measured values for accuracy evaluation.

The structure-based method is a commonly used method for extracting maize structural parameters [18], [23], [24], [26], [37]. Laplacian-based contraction can be used to convert the contracted point cloud into a curve skeleton, via local Delaunay triangulation and topological thinning. In the structure-based method [Fig. 4(b)], the skeleton of the maize plant was first extracted using the open-source code of

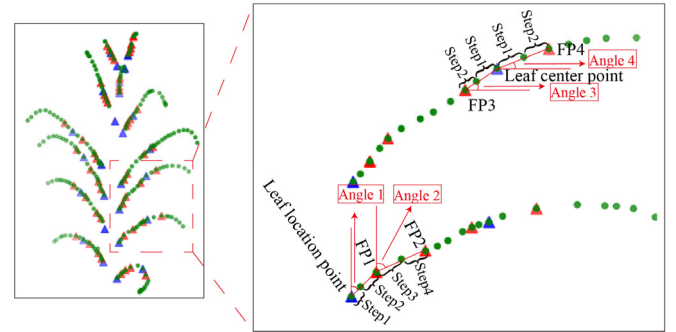


Fig. 5. FPs of each leaf in the structure-based method.

“skeleton-demo” [26]; then, the leaves and stems were separated and individual leaves were acquired to extract the location points and the center points. Finally, because adjacent points in the extracted skeleton points show identical attributes, feature points (FPs) 1–4 (Fig. 5 and Table I) were extracted according to the leaf location point and the leaf center point. Leaf location point with FP1 can be used to calculate Angle 1, while FP1 with FP2 can be used to calculate Angle 2; the average of them is the leaf base angle. Similarly, the leaf inclination angle was calculated using the leaf center point, FP3, and FP4.

C. Separation of Leaves and Stems and Leaf Clustering

1) *Separation of Leaves and Stems*: Leaves and stems separation is a prerequisite for precise phenotypic trait extraction [34], [38]–[42]. The quantitative structure model (QSM) has been used to separate individual leaves from the stems of maize. QSM allows to convert a 3-D point cloud data into a realistic model of a plant for quantitative description of its basic topological structure (e.g., the branch structure), geometry, and volume properties. The QSM reconstruction

TABLE I
DESCRIPTION OF FPs USED IN THE STRUCTURE-BASED METHOD

Feature points	Description
FP1	FP1 represents the feature point that is two steps away from the leaf location point
FP2	FP2 represents the feature point that is four steps away from the leaf location point and two steps away from FP1
FP3	FP3 represents the feature point that is two steps away from the leaf center point and moves towards the leaf location point
FP4	FP4 represents the feature point that is two steps away from the leaf center point and moves away from the leaf location point

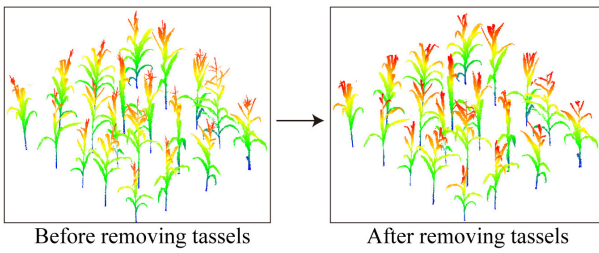


Fig. 6. Point clouds of maize plants before and after tassel removal.

method uses a “cover set” approach, where the point cloud is partitioned into small sets corresponding to small patches on the surface of the maize plant. The optimization method depends on the number of optimized parameters [27], [43], [44], of which the most meaningful are: PatchDiam2Max, PatchDiam2Min, and l cyl. The size of the cover sets is thus controlled by PatchDiam2, *PatchDiam2Max* represents the maximum patch diameter of the cover sets, and *PatchDiam2Min* represents the minimum patch diameter of the cover sets. L cyl represents the relative (length/radius) length of the cylinders, which is used for model reconstruction.

A limitation of the application of QSM to maize plants is that the tassels, which were about 30 cm long, are often mistakenly divided into leaves. To overcome it, during the spinning growth period (*R1*), the point cloud of 30 cm above each maize plant was removed. Then, QSM was used to separate the leaves from the stems (Fig. 6).

2) *Leaf Clustering*: Density-based spatial clustering of applications with noise (DBSCAN) is a density-based clustering algorithm, which can divide areas with high point density into clusters and find clusters of arbitrary shapes in noisy data [38], [45], [46]. The DBSCAN algorithm is sensitive to two clustering parameters: 1) epsilon (Eps), which represents the range of a circular neighborhood centered at a given point *P*, and 2) minpoints (MinPts), the minimum number of points in the neighborhood centered on *P*.

According to the statistical characteristics of the dataset, this study selected clustering parameters based on the *k*-distance method. First, the distances between the objects were calculated using (4) to obtain the distance matrix $\text{Dist}_{n \times n}$

$$\text{Dist}_{n \times n} = \{\text{dist}(i, j), 1 \leq i \leq n, 1 \leq j \leq n\} \quad (4)$$

where *n* is the number of data objects in dataset *D*, and each element represents the distance from Object *i* to Object *j*.

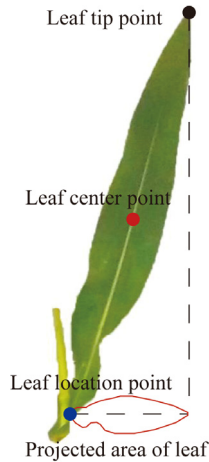


Fig. 7. Geometric features used to extract the leaf base angle and the leaf inclination angle.

Second, each column in the matrix was sorted in ascending order, where column *i* represents the distance between the *i*th point and other points and the *k*th row represents the set of the *k*th distance values nearest to each point.

D. Calculation of Geometric Features

After separating the leaves from the stems and performing leaf clustering, five geometric features were extracted from each individual leaf for estimation of the leaf base and inclination angles: the leaf location point, the leaf center point, the leaf tip point, the number of leaf points, and the projected area of the leaf (Fig. 7). Among them, the leaf location point, center point, and tip point represent the basic shape of a leaf, while the number of leaf points and the projected area can further represent the degree to which the leaf is bent, and their combination can be used to extract the leaf base and inclination angles in a more precise way.

Due to the influence of the natural environment and the growth of the ears, most maize stems do not grow perpendicularly to the ground, and they often bend in the middle and upper parts of the stems. To find a fitted line of the stem, the stem was sliced into different layers. According to an internode length of about 15–20 cm, in this study, a thickness of 15 cm was used for layering. Then, the midpoint of each layer was calculated using the following equation:

$$\begin{cases} (x_{\max} - x_{\min})/2 \\ (y_{\max} - y_{\min})/2 \\ (z_{\max} - z_{\min})/2 \end{cases} \quad (5)$$

Finally, a least squared fitting was used to fit the midpoint of each layer according to

$$\begin{cases} y = a_0 + a_1 x \\ a_0 = \frac{(\sum x_i^2)(\sum y_i) - (\sum x_i)(\sum x_i y_i)}{N(\sum x_i^2) - (\sum x_i)^2} \\ a_1 = \frac{N(\sum x_i y_i) - (\sum x_i)(\sum y_i)}{N(\sum x_i^2) - (\sum x_i)^2} \end{cases} \quad (6)$$

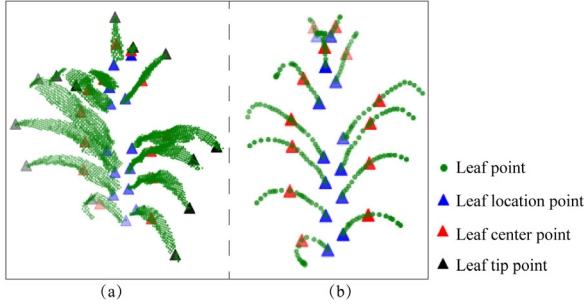


Fig. 8. Leaf location points, leaf center points, and leaf tip points of maize. (a) FPs of maize. (b) FPs of the maize skeleton points.

where x_{\max} and x_{\min} , y_{\max} and y_{\min} , and z_{\max} and z_{\min} are the maximum and minimum values of the coordinates x , y , and z of each point in each layer, respectively, and (x_i, y_i) is the center point coordinates of each layer.

1) FPs Extraction:

a) *Leaf location point*: It is defined as the spatial coordinate of the intersection point of the leaf midrib and the maize stem, which is a useful and frequently measured trait in agronomic research [47]. The leaf point cloud (x , y , z) was used to find the distance (d_1) from each point to the fitted line of the stem. The leaf location point is the leaf point corresponding to the minimum distance. The distance can be calculated as follows:

$$d_1 = \frac{|a_1x - y + a_0|}{\sqrt{a^2 + 1}}. \quad (7)$$

b) *Leaf center point*: It is defined as the spatial coordinate of the center point of the leaf. The coordinates of all the leaf points were arranged in order of their locations and the coordinate of the center point was selected.

c) *Leaf tip point*: It is defined as the spatial coordinate of the tip point of the leaf. The leaf point (x , y , z) is found as the distance (d_2) of each point to the leaf location point (x_l , y_l , z_l); the leaf point corresponding to the maximum distance is the leaf tip point, which is calculated as

$$d_2 = \sqrt{(x - x_l)^2 + (y - y_l)^2 + (z - z_l)^2}. \quad (8)$$

Leaf location points, leaf center points, leaf tip points, and leaf points of maize are shown in Fig. 8.

2) *Leaf Projected Area Calculation*: The projected area of a leaf is defined as the area where the leaf is projected to the ground from the zenith. Each leaf point was projected on a 2-D plane ($z = 0$). A concave polygon can be formed by connecting the outermost points using the k -nearest neighbors approach, where the value of k , the only algorithm parameter, is used to control the “smoothness” of the final solution [48]. The concave hull algorithm was used to find the projected leaf boundaries (Fig. 9). The triangulation arithmetic was used to calculate the leaf projected area according to

$$S = \frac{1}{2} \sum_{i=1}^n (X_i * Y_{i+1} - X_{i+1} * Y_i). \quad (9)$$

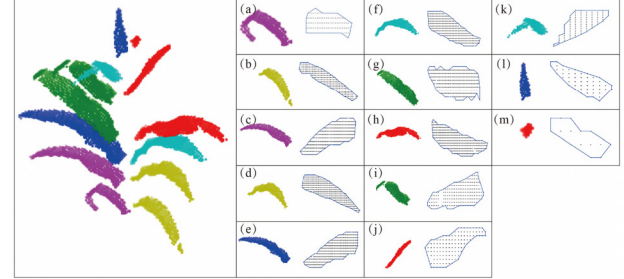


Fig. 9. Concave hull algorithm for projected leaf boundaries. (a)–(m) Different leaves and their projected leaf boundaries.

E. Accuracy Evaluation

To explore the performance of the proposed method for extracting leaf base and inclination angles, we conducted a series of experiments on the dataset of the point cloud.

The precision (P), recall (R), and separation accuracy (SA) served as evaluation metrics to evaluate the leaves and stems separation [49]. These are given by

$$P = \frac{\text{TP}}{\text{TP} + \text{FP}} \quad (10)$$

$$R = \frac{\text{TP}}{\text{TP} + \text{FN}} \quad (11)$$

$$\text{SA} = \frac{\text{TP} + \text{TN}}{\text{TP} + \text{FN} + \text{FP} + \text{TN}}. \quad (12)$$

In (10)–(12), TP, FP, FN, and TN are the total number of true positive, false positive, false negative, and true negative point cloud data, respectively. True positive is a point that is a leaf point and separated into leaf points, false positive is a point that is a leaf point separated into stem points, false negative is a point that is a stem point separated into leaf points, and true negative is a point that is a stem point separated into stem points.

The mean absolute error (MAE), root-mean-squared error (RMSE), and relative root-mean-squared error (rRMSE) were used as the evaluation metrics to assess the accuracy of leaf base and inclination angles. These metrics were calculated as

$$\text{MAE} = \frac{1}{n} \sum_{i=1}^n |x_i - f_i| \quad (13)$$

$$\text{RMSE} = \sqrt{\frac{1}{n} \sum_{i=1}^n (x_i - f_i)^2} \quad (14)$$

$$\text{rRMSE} = \frac{\text{RMSE}}{\bar{x}} \times 100\%. \quad (15)$$

IV. RESULTS

A. Point Cloud Thinning Effect

One uncertainty in the estimation of leaf base and inclination angles is caused by the thinning parameters. According to the point cloud data thinning algorithm, two parameters were used to thin the point cloud data of the maize plants: the voxel size and the number of points in a voxel. Different voxel sizes determine whether the detailed features of a maize plant structure can be retained; a large voxel size may fail to retain the structure information of maize, but a small voxel size requires high computational power. Therefore, a reasonable voxel size

TABLE II
POINT NUMBERS OF A MAIZE PLANT WITH DIFFERENT VOXEL SIZES AND THINNING PARAMETERS

Voxel sizes Times	Original	0.05	0.075	0.1	0.125
0.5	400000	199790	199897	199928	199947
0.1	400000	39644	39815	39880	39912
0.05	400000	19635	19812	19872	19914

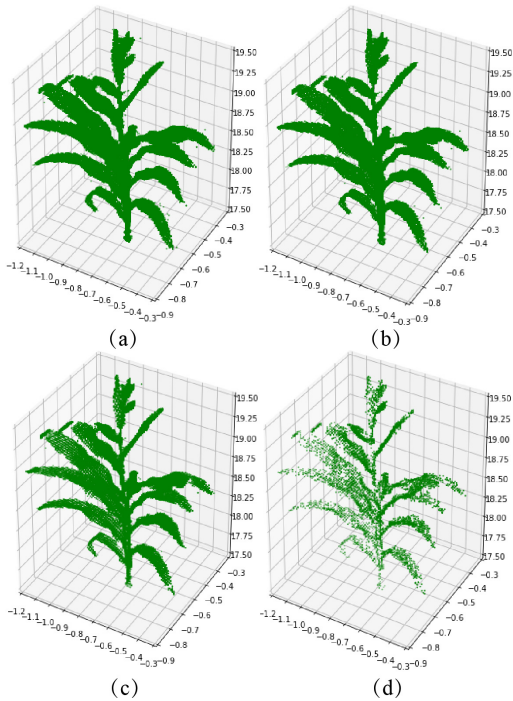


Fig. 10. Thinning parameters effect. (a) Original point clouds. (b) Point clouds with a fraction of 1/2. (c) Point clouds with a fraction of 1/10. (d) Point clouds with a fraction of 1/20.

is required to preserve the maize structure information as well as to guarantee the data processing efficiency. The number of points in a voxel determines the density of the point cloud. Different parameters can influence the extraction of leaf base and inclination angles. Therefore, the effect of the thinning parameters on leaf base and inclination angles was analyzed by calculating the MAE, RMSE, and rRMSE. The voxel sizes of 0.05, 0.075, 0.1, and 0.125 m were used to thin the point cloud of maize plants, and the number of points in the voxel with fractions of 1/2, 1/10, and 1/20 was tested.

Table II shows the point numbers of a maize plant with different voxel sizes and thinning parameters. We can conclude that different voxel sizes have little effect on the point cloud density. For a voxel with the given size of 0.05 m, the point cloud was thinned by reducing the number of points in the voxel with fractions of 1/2, 1/10, and 1/20. Fig. 10(a) shows the original point cloud data and Fig. 10(b) shows the point cloud with a fraction of 1/2. The number of the point cloud was reduced to half of the original one and the detailed features of the maize plant were completely retained; Note that its density was still high. Fig. 10(c) shows the point cloud with a fraction of 1/10, and the detailed features of maize were still retained. Fig. 10(d) shows the point cloud with a fraction of 1/20, and the point cloud density obviously decreased, but the detailed

features of maize were lost. Therefore, the point cloud with a fraction of 1/10 was selected in this study.

Table III lists the accuracy of the estimated leaf angles with different voxel sizes using the thinned point cloud with a fraction of 1/10. It is clear that the accuracy of leaf base and inclination angles decreased with the increase of the voxel size. Therefore, the optimal voxel size of 0.05 m was used in this study.

B. Results for Leaf and Stem Separation

In this study, we first separated the leaves from the stems as this is an important prerequisite for extracting leaf base and inclination angles. High-precision separation of leaves and stem can accurately extract the leaf location points of leaves and further improve the extraction accuracy of leaf base and inclination angles.

Parameters PatchDiam2Max, PatchDiam2Min, and lcy1 were optimized through comparison and analysis and set to 0.06, 0.02, and 1 m, respectively.

The separation results for the 20 maize plants were assessed both visually and quantitatively. Fig. 11 shows the results for leaves and stems separation of the 20 maize plants, which included five varieties and four planting densities. Visually, the results of leaves and stems separation appear correct. However, some misclassifications can be observed in: 1) the part of leaves next to the stem (e.g., those indicated by black rectangles); 2) the top leaves close to the stem (e.g., those indicated by blue circles); and 3) the leaves intersected with each other (e.g., those indicated by red ovals). Quantitatively, the overall separation accuracy of leaves from stems ranged from 0.91 to 0.97, and the precision and recall ranged from 0.92 to 0.99 and 0.87 to 0.96, respectively.

C. Results for Leaf Clustering

In order to observe the statistical characteristics of the dataset at different k values, the distance values ranked the second to the tenth were selected. Fig. 12 shows the distance distribution frequency at different k values at 0.01-m intervals. Because there were different varieties of maize in this study and the morphology of different varieties of maize is quite diverse, each variety of maize was selected. According to the characteristics of each dataset, clustering parameters were selected synthetically.

The distance distribution followed a Poisson curve independently of the k value. When the distance was increased to 0.03 m, the probability density almost decreased to 0. Therefore, the Eps was determined to be 0.03 m. The selection of MinPts was based on the principle of $\text{MinPts} \geq \text{dim} (\text{dimension}) + 1$. In this study, $\text{MinPts} \geq 4$. The MinPts was adjusted according to the clustering results and the Eps value ($\text{Eps} = 0.03$ m). The clustering results of various maize varieties are shown in Fig. 13.

D. Extraction of Maize Leaf Base and Inclination Angles in the Fields

1) Individual Segmentation of Maize From TLS Data: In contrast to maize leaves which tend to intersect as a result of competition for sunlight, the bottoms of stems are naturally

TABLE III
LEAF ANGLE ACCURACY WITH DIFFERENT VOXEL SIZES

Voxel size (m)	Leaf base angle			Leaf inclination angle		
	MAE	RMSE	rRMSE	MAE	RMSE	rRMSE
0.05	4.56°	6.17°	0.19	7.95°	10.00°	0.20
0.075	5.16°	6.92°	0.22	8.51°	10.65°	0.22
0.1	5.40°	7.20°	0.23	8.14°	10.15°	0.20
0.125	5.93°	7.95°	0.25	8.22°	10.23°	0.21

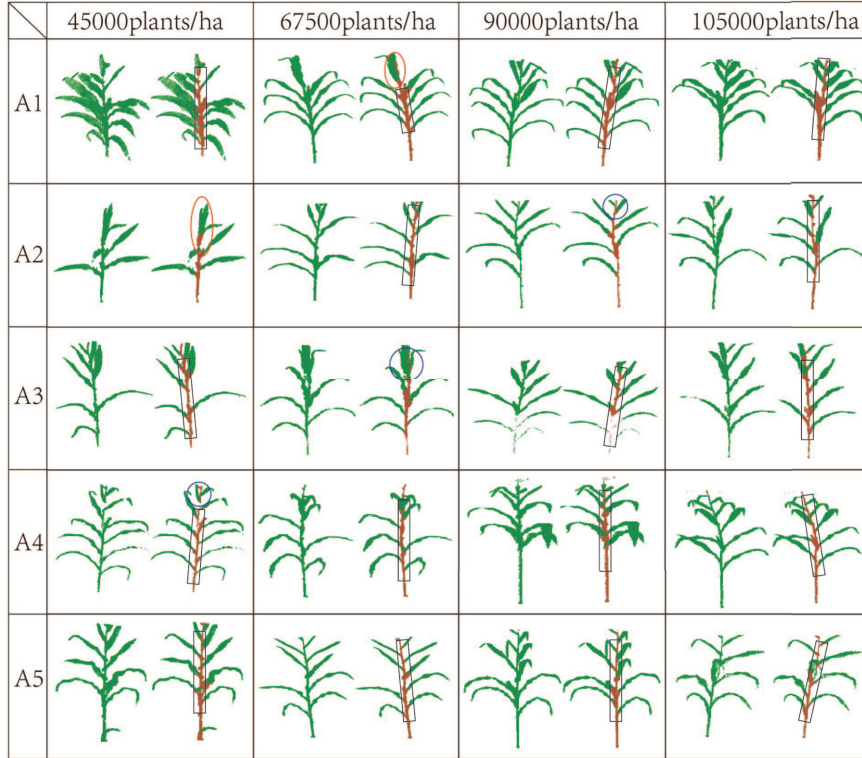


Fig. 11. Results of leaves and stems separation. Stems are shown in brown and leaves in green.

separated from each other and can be accurately detected. As shown in Fig. 14(a1), two slices in the bottom of maize were acquired and the DBSCAN was used for stem location detection, and the union of the two slices was treated as seed points to grow each maize from bottom to up by using the comparative shortest path (CSP) regional growth method proposed by Tao *et al.* [50]. In this study, the maize point cloud severely lacked the details in the internal of the plot because the maize canopy was interlocked and overlapping (the maize planting density is 45 000 plants/ha and the maize is at the filling stage). Fig. 14(b2) and (c2) shows the results of the whole plot and the individual maize segmentation in the boundary of the plot, respectively. At the individual level, 75% of maize plants can be segmented accurately.

2) *Extraction Geometric Features of Maize Leaf:* In this study, only the maize in the boundary was used to extract the leaf base and inclination angles [Fig. 14(c2)] because the maize lacked the details in the internal of the plot. After the separation of leaf and stem, the DBSCAN was used for individual leaf clustering. However, as shown in Fig. 15(a1)–(g1), there are misclassified points because adjacent maize leaves

heavily intersected. When the individual leaf clusters, the clustering shall be removed if the number of points in the cluster is less than 50 [Fig. 15(a2)–(f2)]. Thus, according to the optimized results of clustering, five geometric features (the leaf location point, the leaf center point, the leaf tip point, the number of leaf points, and the projected area of the leaf) were extracted for the estimation of leaf base and inclination angles [Fig. 15(a3)–(g3)].

E. Accuracy of Leaf Base and Inclination Angles Extraction

We compared the TLS extracted leaf base and inclination angles with the measured leaf base and inclination angles to evaluate the accuracy of the proposed methods.

In the machine learning-based method, of the 179 leaves available from the 20 maize plants, 70% were used for training and 30% were used for validation. The proposed machine learning-based methods worked well for the leaf base angles, with MAE = 4.56°, RMSE = 6.17°, and rRMSE = 19.04%, and for the leaf inclination angles, the accuracy remains well with MAE = 7.95°, RMSE = 10.00°, and rRMSE = 20.24%.

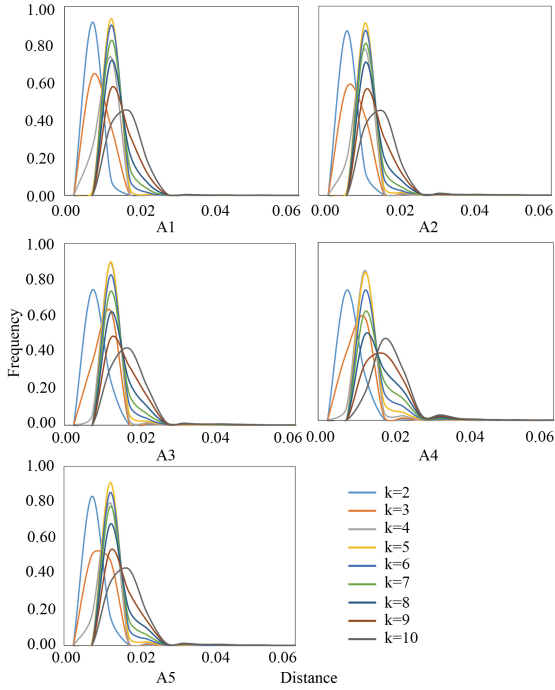


Fig. 12. Frequency of distance distribution against different k values for different maize varieties: A1–A5 are Zhengdan 958, Xianyu 335, Jingnongke 728, Chengdan 30, and Jingpin six varieties, respectively.

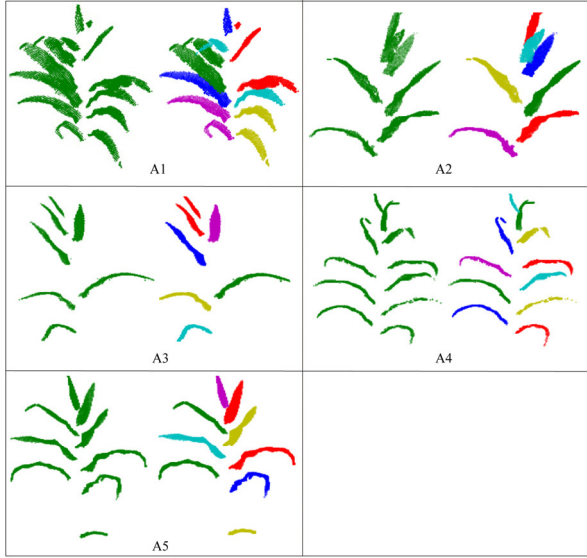


Fig. 13. Clustering results for different maize varieties: A1–A5 are Zhengdan 958, Xianyu 335, Jingnongke 728, Chengdan 30, and Jingpin six varieties, respectively.

To evaluate the structure-based method, we used the same leaves (54 leaves) that were selected for validation in the machine learning-based method so that their performance could be compared with each other. The accuracies of the leaf base and inclination angles were slightly worse than those of the machine learning-based method ($MAE = 6.22^\circ$, $RMSE = 7.47^\circ$, and $rRMSE = 23.30\%$ and $MAE = 8.99^\circ$, $RMSE = 12.57^\circ$, and $rRMSE = 25.85\%$). Table IV shows the comparisons between the machine learning-based method and the structure-based method.

TABLE IV
COMPARISONS BETWEEN THE MACHINE LEARNING-BASED METHOD AND THE STRUCTURE-BASED METHOD

	Parameters	Machine learning-based	Structure-based
Leaf base angles	MAE	4.56°	6.22°
	RMSE	6.17°	7.47°
	rRMSE	19.04%	23.30%
Leaf inclination angles	MAE	7.95°	8.99°
	RMSE	10.00°	12.57°
	rRMSE	20.24%	25.85%

TABLE V
COMPARISONS BETWEEN THE INDIVIDUAL AND THE FIELDS CONDITION OF MAIZE LEAF BASE AND INCLINATION ANGLES

	Parameters	Individual	Field condition
Leaf base angles	MAE	4.56°	6.04°
	RMSE	6.17°	8.12°
	rRMSE	19.04%	25.9%
Leaf inclination angles	MAE	7.95°	11.30°
	RMSE	10.00°	13.52°
	rRMSE	20.24%	26.5%

In the fields, the individual maize was treated as the training set to predict leaf base and inclination angles. The accuracies of the leaf base and the inclination angles were slightly worse than those of the individual maize ($MAE = 6.04^\circ$, $RMSE = 8.12^\circ$, and $rRMSE = 25.90\%$ and $MAE = 11.30^\circ$, $RMSE = 13.52^\circ$, and $rRMSE = 26.5\%$). Table V shows the comparisons between the individual and maize leaf base and inclination angles in the fields by using the machine learning-based method.

V. DISCUSSION

A. Comparisons

1) *Comparison Between the Two Proposed Methods:* In this study, the machine learning-based method and structure-based method were used to extract leaf base and inclination angles. These two methods have some similarities, but they are completely different in nature.

1) The methods are similar as both need to separate the leaves from the stem and perform clustering before the geometric features can be extracted to calculate leaf base and inclination angles.

2) The difference is that the machine learning-based method is based on machine learning, while the structure-based method is based on the plant structure. For the machine learning-based method, geometric features and the real leaf base and inclination angles are used as the training set, and then, the geometric features in the predicted data are used to predict leaf base and inclination angles. For the structure-based method, the skeleton of a maize plant and FPs of the leaves is extracted, and other FPs are extracted according to the connection with the skeleton points. The leaf base and inclination angles are extracted based on the FPs.

The two methods have their advantages and disadvantages. The machine learning-based method is not suitable for small datasets, as it will lead to low accuracy of the leaf base

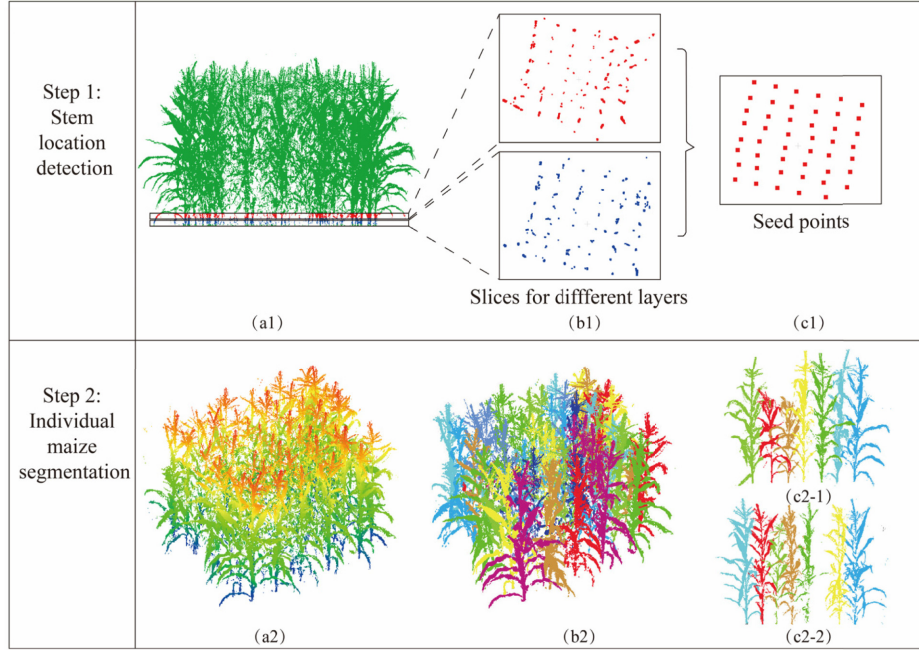


Fig. 14. Individual maize segmentation. Step 1 is the maize location detection. (a1) and (b1) Two slices in the bottom of the maize plants. (c1) Seed points. Step 2 is the CSP regional growth method for individual maize segmentation. (a2) and (b2) Individual maize segmentation of the whole plot. (c2-1) and (c2-2) Individual maize segmentation in the boundary of the plot.

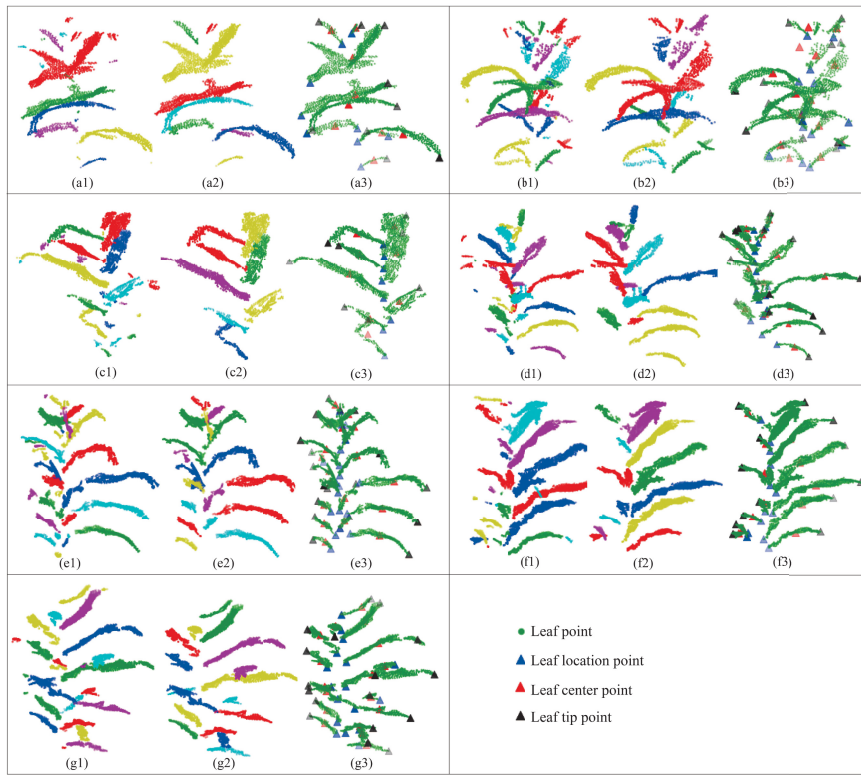


Fig. 15. Leaf clustering and the extraction of geometric features [Fig. 14(c2-1)]. (a1)–(g1) Leaf clustering. (a2)–(g2) Optimized leaf clustering. (a3)–(g3) Leaf location, center and tip points.

and inclination angles. Compared with the machine learning-based method, the structure-based method can extract the leaf base and inclination angles with high accuracy even when the dataset is small, but requires skeleton data, which increases the source of error and reduces the accuracy of leaf base and inclination angles calculation.

2) Comparisons With the Normal Vector-Based Method: The normal vector-based method is a commonly used approach to extract the leaf inclination angle [1], [12], [13], [30]–[33]. Liu *et al.* [32] extracted leaf points, reconstructed leaf surfaces, and then calculated the leaf inclination angles for European beeches. Note that the leaves of European beeches are often

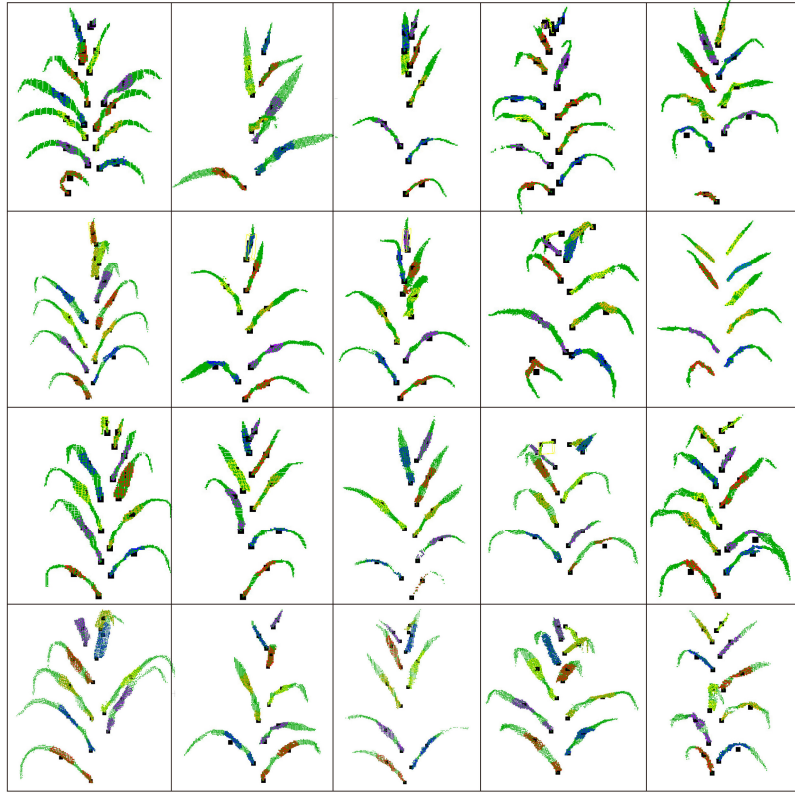


Fig. 16. Normal vector-based method.

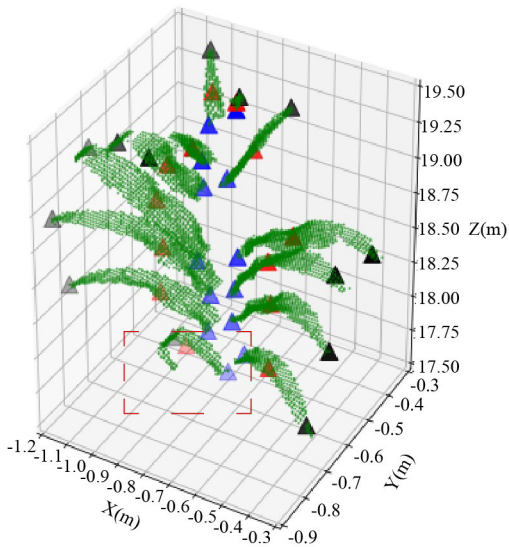


Fig. 17. Leaf tip point extraction error when the leaf is highly bent.

hardly bent. However, in reality, plant leaves, particularly those of maize, are often highly bent, and hence, a simple best-fit plane is not sufficient to represent the leaf orientation. Thus, to properly use this method to estimate the leaf inclination angles, each individual leaf should be divided into a set of small planes.

For the leaf location and center points extracted using the abovementioned methods, let $S = p_i(x, y, z), i \in [1, N_{\text{total}}]$

be the point cloud of a maize leaf, N_{total} be the number of all points, and its neighboring points $N = (p_1, p_2, \dots, p_n)$ be identified by searching all the points in S that are within a given distance L to the leaf location and center points. The results show that the leaf inclination angle was less affected by the change in L (i.e., 0.05, 0.075, 0.1 m in this study), while the leaf base angle gradually changed with the increase of L . The distance of 0.1 m was used for leaf base and inclination angles calculation in this study (Fig. 16). Table VI shows the accuracy comparisons of leaf base and inclination angles between the machine learning- and normal vector-based methods.

B. Factors Affecting the Estimation of Leaf Base and Inclination Angles

Accuracy evaluation carried out on the leaf base and inclination angles shows good agreements with manually measured data and confirmed the good performance of both methods proposed in this work. However, the proposed methods still have some limitations, as discussed next.

Accurate extraction of geometric features of leaves is critical for the estimation of leaf base and inclination angles. Because the leaf tip point is the leaf point corresponding to the maximum Euclidean distance to the leaf location point, when the leaf is highly bent, the leaf tip point cannot be accurately extracted, as shown in Fig. 17, and the situation generally exists in the lower leaf layers.

TABLE VI
COMPARISONS BETWEEN THE MACHINE LEARNING-BASED AND THE NORMAL VECTOR-BASED METHODS

Parameters	Individual maize		Field condition maize	
	Machine learning-based	Normal vector-based	Machine learning-based	Normal vector-based
Leaf base angles	MAE	4.56°	8.72°	6.04°
	RMSE	6.17°	13.33°	8.12°
	rRMSE	19.04%	39.4%	25.9%
Leaf inclination angles	MAE	7.95°	6.03°	11.30°
	RMSE	10.00°	8.71°	13.52°
	rRMSE	20.24%	18.8%	26.5%

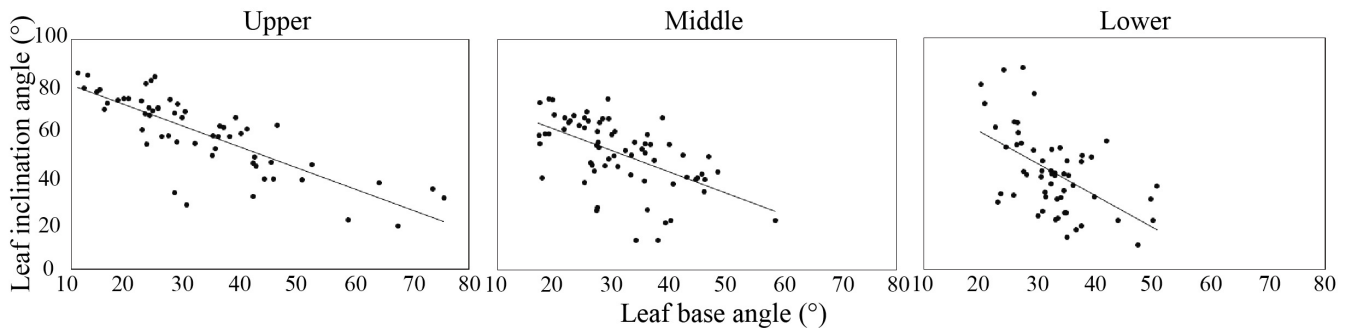


Fig. 18. Relationship between the leaf base and inclination angles of different layers.

TABLE VII
DISTRIBUTION OF LEAF BASE AND INCLINATION ANGLES OF DIFFERENT LAYERS

	Upper	Middle	Lower	
Leaf base angles	Range	10°-80°	15°-50°	20°-50°
	Mode	10°-50°	15°-50°	20°-50°
Leaf inclination angles	Range	10°-90°	10°-75°	10°-90°
	Mode	30°-90°	20°-75°	10°-60°

C. Relationships Between Leaf Base and Inclination Angles

Fig. 18 shows the relationships between leaf base and inclination angles of the upper, middle, and lower layers. If the leaves are not bent, the leaf base and inclination angle are expected to be perfectly complementary, that is, strictly inversely proportional. Therefore, the curvature of the leaf can be further expressed by analyzing the relationships between the leaf base and inclination angles of maize plants.

As can be seen from Fig. 18, from the upper layer to the lower layer, the upper layer has a clear inverse relationship between leaf base and inclination angles. Compared with those of the upper layer, leaf inclination angles of the middle and lower layers are smaller. Because the middle and lower leaves are often wider and larger than the upper leaves, and in order to carry out photosynthesis to a greater extent, leaves will produce a certain degree of curvature, which will affect leaf inclination angles; therefore, the middle and lower layers have slightly worse relationships. In addition, as can be seen from Table VII, in the upper layer, the range of the leaf base angles is greatest (10°–80°), due to the horizontal growth of the upper leaves of the Chengdan 30 variety. It can be seen by analyzing the distribution of the angle ranges and modes (i.e., the most frequent values) for different layers, from upper layers to the

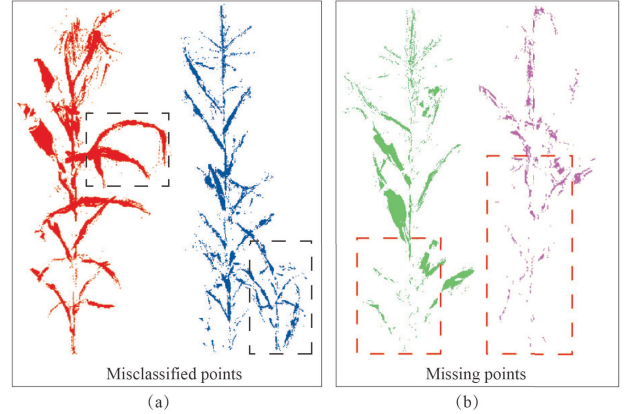


Fig. 19. Misclassified and missing points in the middle of the plot. (a) Misclassified points. (b) Missing points.

lower layers, that the leaf base angle gradually increases as the leaf inclination angle gradually decreases, which improves the absorption of photosynthetic radiation of maize leaves and leads to higher crop yield.

D. Extraction of Maize Leaf Base and Inclination Angles in Fields

Accurate and efficient field crop segmentation methods can rapidly and accurately obtain crop phenotypic traits [52]. After the individual crop is extracted from the plot level, the methods proposed in the study can be used to extract the leaf base and inclination angles of the crop. Researchers have conducted numerous studies on the segmentation of trees [53], [54] and crops [51], [52]. Treeseg [53] first identifies the stem points closer to the ground and the tree is then extracted using generic point cloud processing techniques, including Euclidean

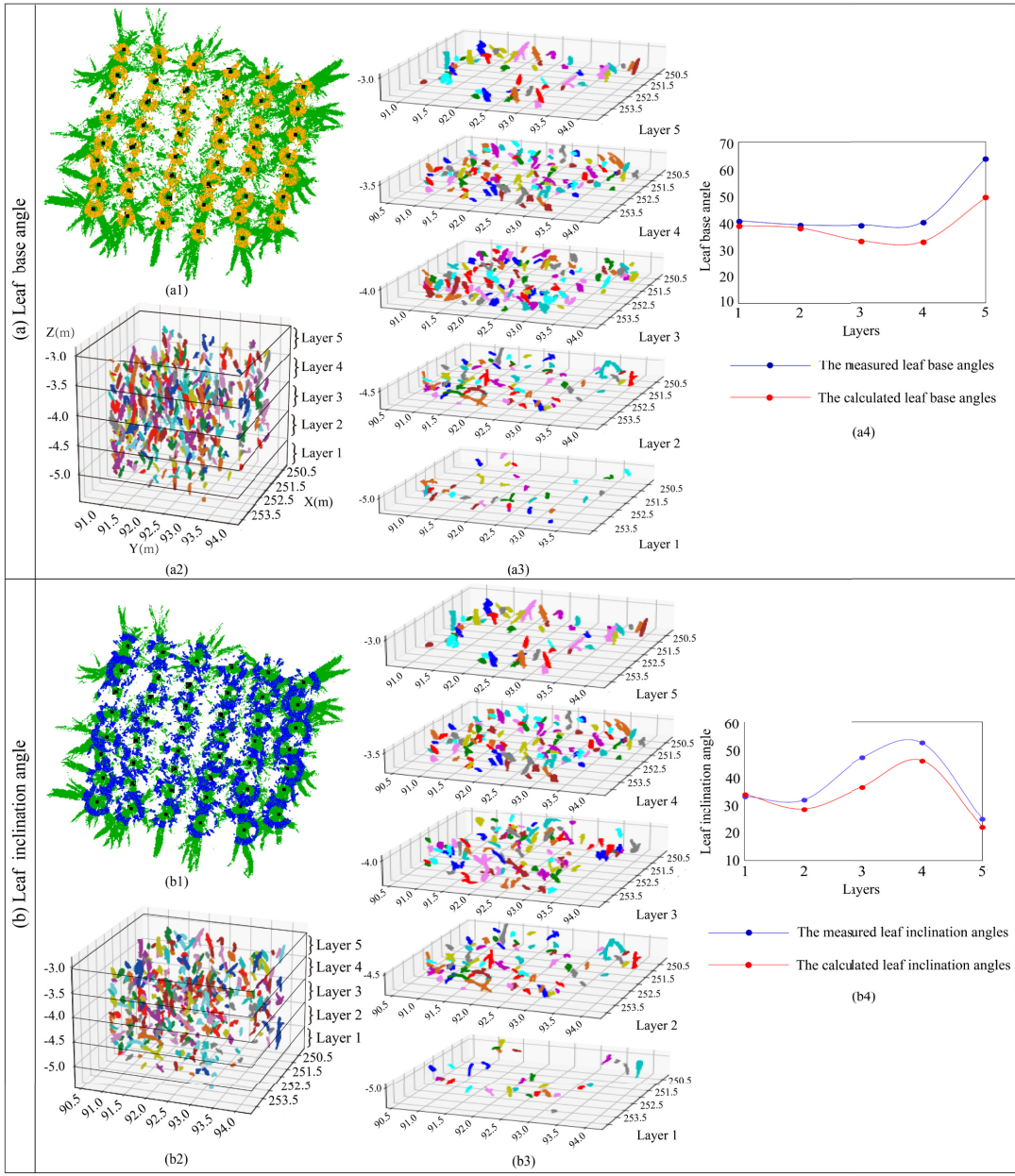


Fig. 20. DBSCAN method was used to extract the leaf base and inclination angles distributions against five layers. (a1) and (b1) Point clouds were extracted for leaf base and inclination angles, respectively (the orange and blue points). (a2) and (b2) DBSCAN method was employed to recognize the clusters. (a3) and (b3) Average leaf base and inclination angles were calculated using the normal vector of five layers with equal heights. (a4) and (b4) Leaf base and inclination angle distributions against layers.

clustering, principal component analysis, region-based segmentation, shape fitting, and connectivity testing. The 3-D FOREST [54] divides the entire forest into horizontal slices, reconstructs the bases of the trees, and adds more clusters to the trees according to the angles and distances between the centroids of the clusters. There have been many studies on individual tree segmentation, but only few previous studies have focused on individual crop segmentation from plot level. Jin *et al.* [51] proposed a method to combine deep learning (Fast R-CNN) and regional growth algorithms to segment individual maize with different planting densities. Li *et al.* [52] developed an individual maize separation approach from top-view images at the seedling stage using the end-to-end segmentation network. In both of the abovementioned previous

studies, the maize was in the seedling stage with limited interlocked and occlusion effects, so it was straightforward to extract individual maize.

In this study, slices in the bottom of maize in the fields were acquired and the DBSCAN was used for stem location detection, which were treated as seed points to grow each maize from bottom to up using the CSP regional growth method proposed by Tao *et al.* [50]. It should be noted that the performance can be degraded with limited TLS observations [55], especially for the maize with highly clustered and overlapping leaves. As shown in Fig. 19, there were missing and misclassified points because the leaves were mutually interlacing and the TLS observations from the lateral side were not able to acquire the details of every single

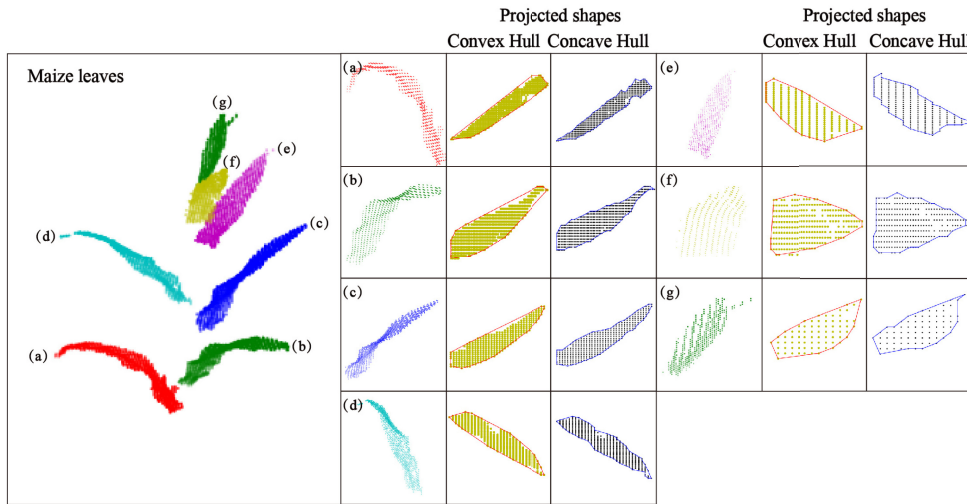


Fig. 21. Individual maize segmentation using regional growth algorithm. (a)–(g) Projected leaf boundaries were extracted using the concave and convex hull algorithms.

maize plot. Registration of multiple terrestrial scans shall be able to obtain the information of the maize plots on the boundary, but considerable information loss can be observed for the internal maize plots, which makes it difficult to extract leaf base and inclination angles using the abovementioned method. Note that the distributions of leaf base and inclination angles are often used to represent the structural characteristics of different maize plants. In this study, the DBSCAN method was employed to recognize the point cloud clusters of the fragmentized leaf blades caused by occlusion, and then, the normal vectors of five layers were calculated to determine the leaf base and inclination angles [56]. To determine the leaf base angles, a hollow cylinder with a thickness of [0.05, 0.15 m] was used to extract point clouds for each seed point [Fig. 20(a1)], and the DBSCAN method was employed to recognize the clusters [Fig. 20(a2)]. The average leaf base angles were calculated using the normal vectors of five layers with equal heights [Fig. 20(a3)], and then, the leaf base angle distributions were determined against layers. Fig. 20(a4) shows that the calculated leaf base angles agreed with the measured angles. A similar procedure was utilized to determine the leaf inclination angles, except that a hollow cylinder with a thickness of [0.15, 0.25 m] was used to extract point clouds [Fig. 20(b1)]. Fig. 20(b4) shows that the calculated and measured leaf inclination angles were also in a good agreement. It should be noted that the differences between the measured and the calculated angles mainly resulted from two factors: 1) the incompleteness of the leaf points caused by occlusion and 2) their different physical representations (i.e., the measured angles represent the maize features at the individual level, while the calculated angles represent the maize features at the plot level).

VI. CONCLUSION

In this study, two methods, i.e., the machine learning-based (SVM-based) method and the structure-based (skeleton extraction-based) method, were utilized to estimate the leaf base and inclination angles of maize plants using TLS.

For the machine learning-based method, leaves and stems were separated based on QSM (overall separation accuracy ranging from 0.91 to 0.97, with precision and recall ranging from 0.92 to 0.99 and from 0.87 to 0.96, respectively), and geometric features (leaf location point, leaf center point, leaf tip point, leaf projected area, and the number of leaf points) were extracted to estimate the leaf base and inclination angles. For the structure-based method, after skeleton extraction, leaves and stems separation, leaf location point, leaf center point, and related FPs were extracted to calculate the leaf base and inclination angles. From the statistical results, we conclude that the following conditions hold.

1) TLS proves to be an effective tool to quantify leaf base and inclination angles due to its capability to acquire massive data rapidly, separation of leaves, and stem points and provide high-precision 3-D information.

2) The machine learning-based method and the structure-based method can extract leaf base and inclination angles accurately. The MAE, RMSE, and rRMSE of the leaf base and inclination angles using the machine learning-based method were 4.56°, 6.17°, and 19.04% and 7.95°, 10.00°, and 20.24%, respectively, and using the structure-based method were 6.22°, 7.47°, and 23.30% and 8.99°, 12.57°, and 25.85%, respectively. The machine learning-based method can also be used to extract leaf base and inclination angles of maize leaf in the fields. The MAE, RMSE, and rRMSE of the leaf base and inclination angles were 6.04°, 8.12°, and 25.90% and 11.30°, 13.52°, and 26.50%, respectively.

3) For different datasets, the two methods have their advantages and disadvantages. The machine learning-based method is suitable for large datasets, while the structure-based method works better on small datasets. In addition, we compared the two presented methods with the normal vector-based method, and the methods presented in this study have an obvious advantage in extracting leaf base angles.

With these new methods, the extinction coefficient can be calculated from the leaf inclination angle to estimate leaf area density (LAD) with the Beer-Lambert law [57], and

TABLE VIII
ACCURACY OF LEAF AND STEM SEPARATION

	Precision	Recall	Accuracy
maize1	0.9970	0.8988	0.9212
maize2	0.9726	0.9135	0.9181
maize3	0.9933	0.8938	0.9205
maize4	0.9939	0.9449	0.9514
maize5	0.9199	0.9554	0.9121
maize6	0.9729	0.8989	0.9083
maize7	0.9758	0.9353	0.9377
maize8	0.9653	0.9121	0.9129
maize9	0.9906	0.9659	0.9678
maize10	0.9951	0.9435	0.9544
maize11	0.9917	0.9308	0.9433
maize12	0.9897	0.9441	0.9510
maize13	0.9616	0.9311	0.9159
maize14	0.9929	0.9736	0.9740
maize15	0.9744	0.9624	0.9531
maize16	0.9938	0.9373	0.9497
maize17	0.9756	0.9656	0.9569
maize18	0.9982	0.8740	0.9022
maize19	0.9796	0.9407	0.9410
maize20	0.9852	0.9262	0.9342

TLS could further serve as a calibration tool for aerial laser scanning (ALS) using the two methods presented in this study. Furthermore, these methods are applicable to other plants and forests to estimate the 3-D structural parameters, such as leaf base and inclination angles. The work presented here will be useful for breeding, which in turn will enable us to better understand the biophysical processes of photosynthesis and evapotranspiration.

APPENDIX

Table VIII shows the separation accuracy, precision, and recall of 20 maize leaves from stems.

Fig. 21 shows maize leaves, and the projected areas with the boundaries extracted using the concave and convex hull algorithms. It appears that the concave hull algorithm can better extract the boundaries of the projected areas.

ACKNOWLEDGMENT

The authors are grateful to the anonymous reviewers for their valuable comments and recommendations.

REFERENCES

- [1] G. Zheng and L. M. Moskal, "Leaf orientation retrieval from terrestrial laser scanning (TLS) data," *IEEE Trans. Geosci. Remote Sens.*, vol. 50, no. 10, pp. 3970–3979, Oct. 2012.
- [2] R. Lemeur and B. L. Blad, "A critical review of light models for estimating the shortwave radiation regime of plant canopies," *Agricul. Meteorol.*, vol. 14, nos. 1–2, pp. 255–286, Jan. 1974.
- [3] R. B. Myneni, "A review on the theory of photon transport in leaf canopies," *Agricul. Forest Meteorol.*, vol. 45, pp. 1–153, Feb. 1989.
- [4] J. Stuckens, B. Somers, S. Delalieux, W. W. Verstraeten, and P. Coppin, "The impact of common assumptions on canopy radiative transfer simulations: A case study in *Citrus* orchards," *J. Quant. Spectrosc. Radiat. Transf.*, vol. 110, nos. 1–2, pp. 1–21, 2009.
- [5] F. Hosoi, Y. Nakai, and K. Omasa, "Estimating the leaf inclination angle distribution of the wheat canopy using a portable scanning LiDAR," *J. Agricul. Meteorol.*, vol. 65, no. 3, pp. 297–302, 2009.
- [6] M. B. Mantilla-Perez and M. G. S. Fernandez, "Differential manipulation of leaf angle throughout the canopy: Current status and prospects," *J. Exp. Botany*, vol. 68, nos. 21–22, pp. 5699–5717, Dec. 2017.
- [7] J. Pisek, O. Sonnentag, A. D. Richardson, and M. Möttus, "Is the spherical leaf inclination angle distribution a valid assumption for temperate and boreal broadleaf tree species?" *Agricul. Forest Meteorol.*, vol. 169, pp. 186–194, Feb. 2013.
- [8] J. Tian *et al.*, "Teosinte ligule allele narrows plant architecture and enhances high-density maize yields," *Science*, vol. 365, no. 6454, pp. 658–664, Aug. 2019.
- [9] S. K. Truong, R. F. McCormick, W. L. Rooney, and J. E. Mullet, "Harnessing genetic variation in leaf angle to increase productivity of *Sorghum bicolor*," *Genetics*, vol. 201, no. 3, pp. 1229–1238, Nov. 2015.
- [10] Z. Ren *et al.*, "ZmILII regulates leaf angle by directly affecting *liguleless1* expression in maize," *Plant Biotechnol. J.*, vol. 18, no. 4, pp. 881–883, Oct. 2019.
- [11] Q. Pan *et al.*, "The genetic basis of plant architecture in 10 maize recombinant inbred line populations," *Plant Physiol.*, vol. 175, no. 2, pp. 858–873, Oct. 2017.
- [12] M. B. Vicari, J. Pisek, and M. Disney, "New estimates of leaf angle distribution from terrestrial LiDAR: Comparison with measured and modelled estimates from nine broadleaf tree species," *Agricul. Forest Meteorol.*, vol. 264, pp. 322–333, Jan. 2019.
- [13] J. Qi, D. Xie, L. Li, W. Zhang, X. Mu, and G. Yan, "Estimating leaf angle distribution from smartphone photographs," *IEEE Geosci. Remote Sens. Lett.*, vol. 16, no. 8, pp. 1190–1194, Aug. 2019.
- [14] J. W. Pendleton, G. E. Smith, S. R. Winter, and T. J. Johnston, "Field investigations of the relationships of leaf angle in corn (*Zea mays* L.) to grain yield and apparent photosynthesis," *Agronomy J.*, vol. 60, no. 4, pp. 422–424, Jul. 1968.
- [15] S. Wagner and M. Hagemeier, "Method of segmentation affects leaf inclination angle estimation in hemispherical photography," *Agricul. Forest Meteorol.*, vol. 139, nos. 1–2, pp. 12–24, Sep. 2006.
- [16] J. Pisek, Y. Ryu, and K. Alikas, "Estimating leaf inclination and G-function from leveled digital camera photography in broadleaf canopies," *Trees*, vol. 25, no. 5, pp. 919–924, Nov. 2011.
- [17] Y. Ryu *et al.*, "How to quantify tree leaf area index in an open savanna ecosystem: A multi-instrument and multi-model approach," *Agricul. Forest Meteorol.*, vol. 150, no. 1, pp. 63–76, Jan. 2010.
- [18] X. Zhang *et al.*, "High-throughput phenotyping and QTL mapping reveals the genetic architecture of maize plant growth," *Plant Physiol.*, vol. 173, no. 3, pp. 1554–1564, Mar. 2017.
- [19] J. Li and L. Tang, "Developing a low-cost 3D plant morphological traits characterization system," *Comput. Electron. Agricult.*, vol. 143, pp. 1–13, Dec. 2017.
- [20] T. Duan, S. C. Chapman, E. Holland, G. J. Rebetzke, Y. Guo, and B. Zheng, "Dynamic quantification of canopy structure to characterize early plant vigour in wheat genotypes," *J. Exp. Botany*, vol. 67, no. 15, pp. 4523–4534, Jun. 2016.
- [21] S. Dandrifosse, A. Bouvry, V. Leemans, B. Dumont, and B. Mercatoris, "Imaging wheat canopy through stereo vision: Overcoming the challenges of the laboratory to field transition for morphological features extraction," *Frontiers Plant Sci.*, vol. 11, p. 96, Feb. 2020.
- [22] D. Zermas, V. Morellas, D. Mulla, and N. Papanikopoulos, "3D model processing for high throughput phenotype extraction—The case of corn," *Comput. Electron. Agricult.*, vol. 172, May 2020, Art. no. 105047.
- [23] S. Jin *et al.*, "Stem–leaf segmentation and phenotypic trait extraction of individual maize using terrestrial LiDAR data," *IEEE Trans. Geosci. Remote Sens.*, vol. 57, no. 3, pp. 1336–1346, Mar. 2019.
- [24] L. Xiang, Y. Bao, L. Tang, D. Ortiz, and M. G. Salas-Fernandez, "Automated morphological traits extraction for sorghum plants via 3D point cloud data analysis," *Comput. Electron. Agricult.*, vol. 162, pp. 951–961, Jul. 2019.
- [25] S. Wu *et al.*, "An accurate skeleton extraction approach from 3D point clouds of maize plants," *Frontiers Plant Sci.*, vol. 10, p. 248, Mar. 2019.
- [26] J. Cao, A. Tagliasacchi, M. Olson, H. Zhang, and Z. Su, "Point cloud skeletons via Laplacian based contraction," in *Proc. Shape Modeling Int. Conf.*, Aix-en-Provence, France, Jun. 2010, pp. 187–197.
- [27] S. Du, R. Lindenbergh, H. Ledoux, J. Stoter, and L. Nan, "AdTree: Accurate, detailed, and automatic modelling of laser-scanned trees," *Remote Sens.*, vol. 11, no. 18, p. 2074, Sep. 2019.
- [28] S. Xiao, S. Liu, K. Bi, and M. Du, "A fast and accurate approach to the extraction of leaf midribs from point clouds," *Remote Sens. Lett.*, vol. 11, no. 3, pp. 255–264, Mar. 2020.
- [29] Y. Li *et al.*, "Retrieval of tree branch architecture attributes from terrestrial laser scan data using a Laplacian algorithm," *Agricul. Forest Meteorol.*, vol. 284, Apr. 2020, Art. no. 107874.
- [30] K. Itakura and F. Hosoi, "Estimation of leaf inclination angle in three-dimensional plant images obtained from LiDAR," *Remote Sens.*, vol. 11, no. 3, p. 344, Feb. 2019.

- [31] Y. Li, Y. Su, T. Hu, G. Xu, and Q. Guo, "Retrieving 2-D leaf angle distributions for deciduous trees from terrestrial laser scanner data," *IEEE Trans. Geosci. Remote Sens.*, vol. 56, no. 8, pp. 4945–4955, Aug. 2018.
- [32] J. Liu *et al.*, "Variation of leaf angle distribution quantified by terrestrial LiDAR in natural European beech forest," *ISPRS J. Photogramm. Remote Sens.*, vol. 148, pp. 208–220, Feb. 2019.
- [33] L. Ma, G. Zheng, J. U. H. Eitel, T. S. Magney, and L. M. Moskal, "Retrieving forest canopy extinction coefficient from terrestrial and airborne LiDAR," *Agricul. Forest Meteorol.*, vol. 236, pp. 1–21, Apr. 2017.
- [34] K. Kuo, K. Itakura, and F. Hosoi, "Leaf segmentation based on k -means algorithm to obtain leaf angle distribution using terrestrial LiDAR," *Remote Sens.*, vol. 11, no. 21, p. 2536, Oct. 2019.
- [35] X. Xu *et al.*, "Wheat ear counting using K -means clustering segmentation and convolutional neural network," *Plant Methods*, vol. 16, no. 1, Aug. 2020, Art. no. 106.
- [36] F. Melgani and L. Bruzzone, "Classification of hyperspectral remote sensing images with support vector machines," *IEEE Trans. Geosci. Remote Sens.*, vol. 42, no. 8, pp. 1778–1790, Aug. 2004.
- [37] S. Wu *et al.*, "An accurate skeleton extraction approach from 3D point clouds of maize plants," *Frontiers Plant Sci.*, vol. 10, Mar. 2019, Art. no. 248.
- [38] R. Ferrara, S. G. P. Virdis, A. Ventura, T. Ghisu, P. Duce, and G. Pellizzaro, "An automated approach for wood-leaf separation from terrestrial LiDAR point clouds using the density based clustering algorithm DBSCAN," *Agricul. Forest Meteorol.*, vol. 262, pp. 434–444, Nov. 2018.
- [39] X. Zhu *et al.*, "Foliar and woody materials discriminated using terrestrial LiDAR in a mixed natural forest," *Int. J. Appl. Earth Observ. Geoinf.*, vol. 64, pp. 43–50, Feb. 2018.
- [40] M. B. Vicari, M. Disney, P. Wilkes, A. Burt, K. Calders, and W. Woodgate, "Leaf and wood classification framework for terrestrial LiDAR point clouds," *Methods Ecol. Evol.*, vol. 10, no. 5, pp. 680–694, Jan. 2019.
- [41] S. M. K. Moorthy, K. Calders, M. B. Vicari, and H. Verbeeck, "Improved supervised learning-based approach for leaf and wood classification from LiDAR point clouds of forests," *IEEE Trans. Geosci. Remote Sens.*, vol. 58, no. 5, pp. 3057–3070, May 2020.
- [42] M. Béland, D. D. Baldocchi, J.-L. Widlowski, R. A. Fournier, and M. M. Verstraete, "On seeing the wood from the leaves and the role of voxel size in determining leaf area distribution of forests with terrestrial LiDAR," *Agricul. Forest Meteorol.*, vol. 184, pp. 82–97, Jan. 2014.
- [43] P. Raumanen *et al.*, "Fast automatic precision tree models from terrestrial laser scanner data," *Remote Sens.*, vol. 5, no. 2, pp. 491–520, Jan. 2013.
- [44] L. Terryn *et al.*, "Tree species classification using structural features derived from terrestrial laser scanning," *ISPRS J. Photogramm. Remote Sens.*, vol. 168, pp. 170–181, Oct. 2020.
- [45] M. Ester, H. P. Kriegel, J. Sander, and X. Xu, "A density-based algorithm for discovering clusters in large spatial databases with noise" in *Proc. Int. Conf. Knowl. Discovery Data Mining*, Portland, OR, USA, Aug. 1996, pp. 226–231.
- [46] J. Sander, M. Ester, H.-P. Kriegel, and X. Xu, "Density-based clustering in spatial databases: The algorithm GDBSCAN and its applications," *Data Mining Knowl. Discovery*, vol. 2, no. 2, pp. 169–194, Jun. 1998.
- [47] C. Guo, G. Liu, W. Zhang, and J. Feng, "Apple tree canopy leaf spatial location automated extraction based on point cloud data," *Comput. Electron. Agricult.*, vol. 166, Nov. 2019, Art. no. 104975.
- [48] A. Moreira and M. Y. Santos, "Concave hull: A k -nearest neighbours approach for the computation of the region occupied by a set of points," in *Proc. Int. Conf. Comput. Graph. Theory Appl.*, Barcelona, Spain, 2007, pp. 61–68.
- [49] Z. Zhihua, *Machine Learning*. Beijing, China: Tsinghua Univ. Press, 2016.
- [50] S. Tao *et al.*, "Segmenting tree crowns from terrestrial and mobile LiDAR data by exploring ecological theories," *ISPRS J. Photogramm. Remote Sens.*, vol. 110, pp. 66–76, Dec. 2015.
- [51] S. Jin *et al.*, "Deep learning: Individual maize segmentation from terrestrial LiDAR data using faster R-CNN and regional growth algorithms," *Frontiers Plant Sci.*, vol. 9, Jun. 2018, Art. no. 866.
- [52] Y. Li *et al.*, "High-throughput phenotyping analysis of maize at the seedling stage using end-to-end segmentation network," *PLoS ONE*, vol. 16, no. 1, Jan. 2021, Art. no. e0241528.
- [53] A. Burt, M. Disney, K. Calders, and S. Goslee, "Extracting individual trees from LiDAR point clouds using *treeseg*," *Methods Ecol. Evol.*, vol. 10, no. 3, pp. 438–445, 2019.
- [54] J. Trochta, M. Kruček, T. Vrška, and K. Král, "3D forest: An application for descriptions of three-dimensional forest structures using terrestrial LiDAR," *PLoS ONE*, vol. 12, no. 5, May 2017, Art. no. e0176871.
- [55] T. Yun *et al.*, "Simulation of multi-platform LiDAR for assessing total leaf area in tree crowns," *Agricul. Forest Meteorol.*, vols. 276–277, Oct. 2019, Art. no. 107610.
- [56] Q. Xu, L. Cao, L. Xue, B. Chen, F. An, and T. Yun, "Extraction of leaf biophysical attributes based on a computer graphic-based algorithm using terrestrial laser scanning data," *Remote Sens.*, vol. 11, no. 1, p. 15, Dec. 2018.
- [57] G. Yan *et al.*, "Review of indirect optical measurements of leaf area index: Recent advances, challenges, and perspectives," *Agricul. Forest Meteorol.*, vol. 265, pp. 390–411, Feb. 2019.



Lei Lei received the B.S. and M.A. degrees from the Xi'an University of Science and Technology, Xi'an, China, in 2017 and 2020, respectively. She is currently pursuing the Ph.D. degree with the College of Geological Engineering and Geomatics, Chang'an University, Xi'an.

She is also a Member of the Big Data Center for Geosciences and Satellites (BDCGS), Xi'an, and a Visiting Student with the Information Technology Research Center, Beijing Academy of Agriculture and Forestry Sciences, Beijing, China. Her research focuses on LiDAR and crop phenotyping.



Zhenhong Li (Senior Member, IEEE) received the B.Eng. degree in geodesy from the Wuhan Technical University of Surveying and Mapping (now Wuhan University), Wuhan, China, in 1997, and the Ph.D. degree in GPS, geodesy, and navigation from University College London, London, U.K., in 2005.

He is currently a Professor of imaging geodesy with the College of Geological Engineering and Geomatics, Chang'an University, Xi'an, China, the Director with the Big Data Center for Geosciences and Satellites (BDCGS), Xi'an, and the Director of the Key Laboratory of Western China's Mineral Resource and Geological Engineering, Ministry of Education, Xi'an. He is also a Visiting Professor with the School of Engineering, Newcastle University, Newcastle upon Tyne, U.K. He is also the Principal Investigator of the Generic Atmospheric Correction Online Service (GACOS) for interferometric synthetic aperture radar. His research interests include space geodesy and remote sensing (mainly InSAR and GNSS) and their applications to geohazards (e.g., earthquakes, landslides, and land subsidence), and precision agriculture.

Dr. Li is a fellow of the International Association of Geodesy and an Associate Editor of Advances in Space Research and Remote Sensing.



Jintao Wu received the Ph.D. degree in computer science and technology from Anhui University, Hefei, China, in 2020.

He is currently a Lecturer with the School of Computer and Software, Nanjing University of Information Science and Technology, Nanjing, China. His research interests include service computing, cloud computing, and computer vision.



Chengjian Zhang received the B.S. and M.A. degrees from the Xi'an University of Science and Technology, Xi'an, China, in 2018 and 2021, respectively. He is currently pursuing the Ph.D. degree with the School of Information Science and Technology, Beijing Forestry University, Beijing, China.

He is also a Visiting Student with the Information Technology Research Center, Beijing Academy of Agriculture and Forestry Sciences, Beijing. His research interest includes LiDAR-based fruit tree application.



Zhen Dong received the B.S. degree in engineering from the Shandong University of Science and Technology, Qingdao, China, in 2018. He is currently pursuing the M.S. degree with the College of Geodesy and Geomatics, Shandong University of Science and Technology, Qingdao.

He is also a Visiting Student with the Information Technology Research Center, Beijing Academy of Agriculture and Forestry Sciences, Beijing, China. His research interests include remote sensing and agronomy to achieve the calculation of vertical light distribution of crops.



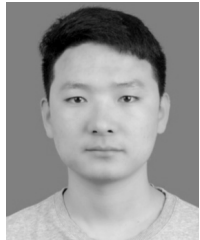
Yaohui Zhu received the M.S. degree in agriculture from Henan Agricultural University, Zhengzhou, China, in 2018. He is currently pursuing the Ph.D. degree with the School of Information Science and Technology, Beijing Forestry University, Beijing, China.

He is also a Visiting Student with the Information Technology Research Center, Beijing Academy of Agriculture and Forestry Sciences, Beijing. His research interests include remote sensing and meteorology to solve the challenges of precise orchard management.



Hao Yang received the M.A. degree from the Chinese Academy of Sciences Center for Earth Observation and Digital Earth Science, Beijing, China, in 2009, and the Ph.D. degree from the Resource Information Institute, Chinese Academy of Forestry, Beijing, in 2015.

He is currently an Associate Professor with the Information Technology Research Center, Beijing Academy of Agriculture and Forestry Sciences, Beijing. His research interests include phenotyping and agricultural remote sensing.



Riqiang Chen received the B.S. degree from the Henan University of Engineering, Zhengzhou, China, in 2018, the M.S. degree from the School of Surveying and Land Information Engineering, Henan Polytechnic University, Jiaozuo, China, in 2021. He is currently pursuing the Ph.D. degree with the School of Information Science and Technology, Beijing Forestry University, Beijing, China.

He is also a Visiting student with the Information Technology Research Center, Beijing Academy of Agriculture and Forestry Sciences, Beijing. His research interest includes LiDAR-based fruit tree application.



Guojun Yang received the Ph.D. degree in cartography and geography information system from the Institute of Remote Sensing Applications, Chinese Academy of Sciences, Beijing, China, in 2008.

He is currently a Professor with the Information Technology Research Center, Beijing Academy of Agriculture and Forestry Sciences, Beijing, and the Director with the Key Laboratory of Quantitative Remote Sensing in Agriculture of Ministry of Agriculture and Rural Affairs, Beijing. He mainly engages in radiative transfer modeling and quantitative remote sensing in agriculture and forestry.